Spectral behavior of thin film coated cascaded tapered long period gratings in multiple configurations

P. Pilla[1,2], P. Foglia Manzillo[1], M. Giordano[2], M. L. Korwin-Pawlowski[3], W. J. Bock[4] and A. Cusano[1]

[1]*Optoelectonic Division, Engineering Department, University of Sannio, Benevento, Italy.*
[2]*Institute for Composite and Biomedical Materials, National Research Council (IMCB-CNR), Napoli, Italy.*
[3]*Département d'informatique et d'ingénierie, Université du Québec en Outaouais, Gatineau, Canada.*
[4]*Centre de recherche en photonique, Université du Québec en Outaouais, Gatineau, Canada.*
Corresponding author: pillapie@unisannio.it

Abstract: In this work the spectral response of cascaded tapered long period gratings coated by nano-sized polymeric films has been investigated as function of the surrounding medium refractive index (SRI). The investigation was aimed to identify the best configuration in terms of coated/not coated areas in order to fully benefit of the SRI sensitivity enhancement due to the modal transition mechanism of nano-coated long period gratings while preserving the fringes visibility.

OCIS codes: (050.2770) Gratings; (120.3180) Interferometry; (060.2370) Fiber optics sensors; (120.0280) Polymers; (310.1860) Deposition and fabrication.

References and links

1. S. W. James and R. P. Tatam, "Optical fibre long-period grating sensors: characteristics and application," Meas. Sci. Technol. **14**, R49-R61 (2003).
2. S. W. James and R. P. Tatam, "Fibre Optic Sensors with Nano-Structured Coatings," J. Opt. A **8**, S430-S444 (2006).
3. S. W. James, N. D. Rees, G. J. Ashwell, and R. P. Tatam, "Optical fibre long period gratings with Langmuir Blodgett thin film overlays," Opt. Lett. **9**, 686–688 (2002).
4. I. Del Villar, M. Achaerandio, I. R. Matías, and F. J. Arregui, "Deposition of an Overlay with Electrostactic Self-Assembly Method in Long Period Fiber Gratings," Opt. Lett. **30**, 720-722 (2005).
5. A. Cusano, A. Iadicicco, P. Pilla, L. Contessa, S. Campopiano, A. Cutolo, and M. Giordano, "Mode transition in high refractive index coated long period gratings," Opt. Express **14**, 19-34 (2006).
6. A. Cusano, A. Iadicicco, P. Pilla, A. Cutolo, M. Giordano, and S. Campopiano, "Sensitivity characteristics in nanosized coated long period gratings," Appl. Phys. Lett. **89**, 201116- (2006).
7. A. Cusano, A. Iadicicco, P. Pilla, L. Contessa, S. Campopiano, A. Cutolo, and M. Giordano, "Cladding mode reorganization in high-refractive-index-coated long-period gratings: effects on the refractive-index sensitivity," Opt. Lett. **30**, 2536-2538 (2005).
8. A. Cusano, A. Iadicicco, P. Pilla, L. Contessa, S. Campopiano, A. Cutolo, M. Giordano, and G. Guerra, "Coated Long-Period Fiber Gratings as High-Sensitivity Optochemical Sensors," J. Lightwave Technol. **24**, 1776- (2006).
9. J. Lee, Q. Chen, Q. Zhang, K. Reichard, D. Ditto, J. Mazurowski, M. Hackert, and S. Yin, " Enhancing the tuning range of a single resonant band long period grating while maintaining the resonant peak depth by using an optimized high index indium tin oxide overlay," Appl. Opt. **46**, 6984-6989 (2007).
10. I. D. Villar, I. R. Matias, F. J. Arregui, and M. Achaerandio, "Nanodeposition of Materials With Complex Refractive Index in Long-Period Fiber Gratings," J. Lightwave Technol. **23**, 4192- (2005).
11. I. K. Hwang, S. H. Yun, and B. Y. Kim, "Long-period fiber gratings based on periodic microbends," Opt. Lett. **24**, 1263-1265 (1999).
12. D. D. Davis, T. K. Gaylord, E. N. Glytis, and S. C. Mettler, **"**CO2 laser-induced long-period fibre gratings: spectral characteristics, cladding modes and polarization independence," Electron. Lett. **34**, 1414-1417 (1998).
13. G. Rego, O. Okhotnikov, E. Dianov, and V. Sulimov, "High-temperature stability of long period fiber gratings produced using an electric arc," J. Lightwave Technol. **19**, 1574-1579 (2001).

#91780 - $15.00 USD Received 15 Jan 2008; revised 13 Mar 2008; accepted 15 Mar 2008; published 18 Jun 2008

14. W. J. Bock, J. Chen, P. Mikulic, T. Eftimov, and M. Korwin-Pawlowski, "Pressure sensing using periodically tapered long-period gratings written in photonic crystal fibers," Meas. Sci. Technol. **18**, 3098-3102 (2007).
15. P. Pilla, M. Giordano, M. L. Korwin-Pawlowski, W. J. Bock, and A. Cusano, "Sensitivity Characteristics Tuning in Tapered Long-Period Gratings by Nanocoatings, " IEEE Photon. Technol. Lett. **19**, 1517-1519 (2007).
16. Y.-G. Han, B. H. Lee, W.-T. Han, U.-C. Paek, and Y. Chung, "Fibre-optic sensing applications of a pair of long-period fibre gratings," Meas. Sci. Technol. **12**, 778-781 (2001).
17. R. P. Murphy, S. W. James, and R. P. Tatam, "Multiplexing of Fiber-Optic Long-Period Grating-Based Interferometric Sensors," J. Lightwave Technol. **25**, 825-829 (2007).
18. E. M. Dianov, S. A.Vasiliev, A. S. Kurkov, O. J. Medvedkov, and V. N. Protopopov, "In-fiber Mach-Zehnder interferometer based on a pair of long-period gratings," in Proc. European conf. Optical Communication, 65-68 (1996).
19. A. Cusano, D. Paladino, A. Cutolo, I. Del Villar, I. R. Matias, and F. J. Arregui, "Spectral characteristics in long-period fiber gratings with nonuniform symmetrically ring shaped coatings," Appl. Phys. Lett. **90**, 141105- (2007).
20. I. Del Villar, F. J. Arregui, I. R. Matias, A. Cusano, D. Paladino, and A. Cutolo, "Fringe generation with non-uniformly coated long-period fiber gratings," Opt. Express **15**, 9326-9340 (2007).
21. S. W. James, I. Ishaq, G. J. Ashwell, and R. P. Tatam, "Cascaded long-period gratings with nanostructured coatings," Opt. Lett. **30**, 2197-2199 (2005).
22. G. Rego, O. V. Ivanov, P. V.S. Marques and J. L. Santos "Investigation of Formation Mechanisms of Arc-Induced Long-Period Fiber Gratings," in Proc. of 18th Int. Conf. on Optical Fiber Sensors, Cancun, Mexico, paper TuE84 (2006).
23. D. Marcuse, *Theory of Dielectric Optical Waveguides* (Academic Press, New York, 1974).
24. B. H. Lee, Y.-J. Kim, Y. Chung, W.-T. Han, and U.-C. Paek, "Fibre modal index measurements based on fibre gratings," Fiber Integr. Opt. **20**, 443-455 (2001).
25. H. J. Patrick, A. D. Kersey, and F. Bucholtz, "Analysis of the response of long period fiber gratings to external index of refraction," J. Lightwave Technol. **16**, 1606-1612 (1998).
26. D. W. Kim, Y. Zhang, K. L. Cooper, and A. Wang, "In-fiber reflection mode interferometer based on a long-period grating for external refractive-index measurement," Appl. Opt. **44**, 5368-5373 (2005).
27. I. Del Villar, I. R. Matias, F. J. Arregui, and P. Lalanne, "Optimization of sensitivity in Long Period Fiber Gratings with overlay deposition," Opt. Exp. **13**, 56-69 (2005).
28. M. Giordano, M. Russo, A. Cusano, and G. Mensitieri, "An high sensitivity optical sensor for chloroform vapours detection based on nanometric film of δ-form syndiotactic polystyrene," Sens. Actuators B **107**, 140-147 (2005).
29. L. E. Scriven, "Physics And Applications of Dip Coating And Spin Coating," Mater. Res. Soc. Symp. Proc. **121**, 717-729 (1988).
30. X. Shu, L. Zhang, and I. Bennion, "Sensitivity Characteristics of Long-Period Fiber Gratings," J. Lightwave Technol. **20**, 255- (2002).
31. G. Humbert and A. Malki, " Electric-arc-induced gratings in non-hydrogenated fibres: fabrication and high temperature characterizations," J. Opt. A **4**, 194-198 (2002).
32. R. Falate, G. R. C. Possetti, R. C. Kamikawachi, J. L. Fabris, and H. J. Kalinowski, "Temperature influence of an air conditioner in refractive index measurements using long-period fiber gratings," Third European Workshop on Optical Fibre Sensors, Proc. of the SPIE **6619**, 66193W (2007).
33. M. J. Weber, *Handbook of optical materials* (CRC, New York, 2003).
34. Y. -J. Kim, U. -C. Paek, and B. H. Lee, "Measurement of refractive-index variation with temperature by use of long-period fiber gratings," Opt. Lett. **27**, 1297-1299 (2002).

1. Introduction

In the last years Long Period Gratings (LPGs) have been widely investigated for sensing applications [1]. More recently modification of LPGs spectral properties through deposition of nano-structured coatings onto the grating is attracting an increasingly high interest [2]. Different techniques such as Langmuir-Blodgett (LB), electrostatic self assembly (ESA) and dip-coating have been exploited for the deposition of nano-sized overlays which have shown to produce significant influence on LPGs transmission spectrum and sensitivity characteristics [3-6]. In particular, when azimuthally symmetric nano-scale high refractive index (HRI) coatings are deposited onto LPGs, a significant modification of the cladding modes distribution occurs, depending on the layer features (refractive index and thickness) and on the surrounding medium refractive index (SRI). If layer parameters are properly chosen and the SRI is increased in a certain range, the transition of the lowest order cladding mode into an

#91780 - $15.00 USD Received 15 Jan 2008; revised 13 Mar 2008; accepted 15 Mar 2008; published 18 Jun 2008

overlay mode occurs. As a consequence, a cladding modes re-organization takes place leading to relevant improvements in the SRI sensitivity in terms of wavelength shift and amplitude variations of LPGs attenuation bands [5]. The coated devices have found application as refractive index sensors, chemical sensors and tunable filters [7-9]. Unfortunately LB and ESA techniques, while providing high control of the overlay thickness produce high loss overlays as well, which are in turn responsible for the fading of the attenuation bands exactly in the most sensitive region of the device [10]. On the contrary the dip-coating technique permits to deposit low absorption overlays thus preserving rather well the attenuation bands from the disappearance in the transition region.

LPGs are classically realized by exposing the optical fiber to UV lasers through an amplitude mask, utilizing the photosensitive properties of the fiber. However, even if this is the most commonly and readily used writing method in the industry, it has certain shortcomings as highlighted by Hwang et al. [11]. In particular, a large number of photomasks is required to fabricate gratings with different periods; hydrogen loading is necessary to increase the photosensitivity and to facilitate the refractive index change, and last but not least, UV laser sources are expensive. Recently several non-photosensitive techniques for grating fabrication have been reported either using a CO_2 laser [12] or an electric arc discharge [13]. The inscription mechanism such as physical deformation, stress relaxation or dopant diffusion depend on the type of the fiber used and its maintaining conditions (tension, bending). Some advantages of using the electric arc technique lie in the fact that it needs simple and inexpensive fabrication procedure and equipment; it is a flexible technique and permits to write gratings on any kind of optical fiber, even on pure silica Photonics Crystal Fibers where no germanium core doping or hydrogen loading is applicable [14]. Moreover, this technique provides a higher thermal stability of the device with respect to UV writing methods [13]. Tapered LPGs (TLPGs) are periodically tapered optical fibers realized by means of an electric arc and a pulling weight. The mechanism of the modal transition was demonstrated to take place in coated TLPGs and to enhance the sensitivity of the bare device to SRI changes for a broad range of SRI values [15]. Thin polymeric overlays where deposited onto TLPGs by dip-coating technique which showed to be a reliable technique for the deposition of conformal coatings with the necessary thickness control to tune the transition region in the desired SRI range.

Compound structures realized by using the single LPG as building block and characterized by the presence of finer-scale features within the wide attenuation bands of a single LPG are emerging for the higher sensitivity and resolution offered in the measurement of environmental parameters changes [16,17]. In particular two in series LPGs separated by a few centimeters separation length produce a transmission spectrum with a sinusoidal fringe pattern whose envelope is related to the attenuation bands of the single grating. Such cascaded LPGs have been explained in analogy to a Mach-Zender interferometer [18]. Similar effects have been also observed in the case of non uniform ring shaped nano-coated LPGs [19,20].

Recently, James et al. [21] investigated the effect of LB overlay deposition onto cascaded UV-written LPGs by changing the overlay thickness. They analyzed two configurations: overlay deposited onto the fiber separation length between the two LPGs and overlay deposited along the entire length of the device. In the first case, as the overlay thickness was increased, a blue wavelength shift of the interference fringes minima was observed along with a reduction of the fringes visibility, while the fringe envelope remained unchanged. In the second case, in addition to the change in the phase and visibility of the fringes , a change in the central wavelength and amplitude of the attenuation bands was recorded.

To the purposes of this work a computer-assisted arc-discharge system was used to fabricate cascaded LPGs. Each grating was made of periodic tapers in single-mode Corning SMF-28 optical fibers. Such cascaded tapered LPGs (C-TLPGs) were coated with thin films of Syndiotactic Polystyrene (sPS) by using the dip-coating method. Multiple configurations in terms of coated/not coated areas were realized and a spectral characterization of the devices to the SRI changes was performed. The aim was to extend the experimental observations made

#91780 - $15.00 USD Received 15 Jan 2008; revised 13 Mar 2008; accepted 15 Mar 2008; published 18 Jun 2008

in [21] exploiting the low absorption sPS overlay and, at the same time, to show the good spectral features of C-TLPGs.

2. Theoretical background

The spectral characteristics of single LPGs are determined by coupling between the fundamental guided core mode LP_{01} and the co-propagating cladding modes LP_{0i} when the core propagating light encounters a periodic perturbation of fiber refractive index. From the coupled mode theory the resonant wavelengths at which the transmission spectra present the minima are approximately given by the well known first order Bragg condition [1]:

$$\lambda_{res,0i} = \left(n_{eff,co} - n_{eff,cl}^{0i}\right) \cdot \Lambda \tag{1}$$

Where $n_{eff,co}$ and $n_{eff,cl}^{0i}$ are the core and i^{th} cladding mode effective indices respectively, Λ is the grating period.

In TLPGs the refractive index modulation is achieved by tapering the optical fiber. Although the mechanism of the grating formation is still under dispute [22] some observations enforce the idea that for our gratings the coupling mechanism is prevalently determined by the effective refractive index modulation due to geometric deformation. For example, from SEM analysis it was possible to estimate a bare fiber cross section reduction in the taper waist of about 18% in the case of single gratings. By assuming a constant core/cladding diameter ratio throughout the taper it is possible to infer the core diameter in the waist of the tapered region. The use of the concept of the local normal modes [23] and the solution of the scalar wave equation (linearly polarized modes approximation) [5] in the two different sections of the device permits to evaluate the propagation constants of the core mode in the unperturbed fiber (8.2μm diameter) and in the waist of the taper. Finally, considering that the propagation constants are linked to the effective refractive index by the relation $\beta=(2\pi/\lambda)n_{eff}$, it was possible to estimate an effective refractive index modulation amplitude of about of $6.8*10^{-4}$ (averaged in the spectral range 1400-1700 nm). This is consistent with typical values of the refractive index modulation amplitude in classic UV-written gratings and hence strong enough to induce the mode coupling. However a co-participation of glass stress relaxation and dopant diffusion can not be excluded.

When two LPGs are connected in series separated by a short distance of few centimeters of unperturbed fiber we obtain a device also known as cascaded LPGs whose behavior can be described in analogy to a Mach-Zender interferometer [18]. The first LPG couples light to cladding modes which experience a different optical path with respect to the core mode. At the second LPG the cladding modes are coupled back into the core interfering with the core mode. The transmission spectrum of cascaded LPGs exhibits an envelope corresponding to the attenuation bands normally present for a single LPG and which is sinusoidally modulated by numerous interference fringes. It can be mathematically described by [24]:

$$I = I_{core} + \alpha \cdot I_{clad,i} + 2 \cdot \sqrt{\alpha \cdot I_{core} \cdot I_{clad,i}} \cdot \cos\theta \tag{2}$$

where I_{core} and $I_{clad,i}$ are the intensities of the core mode and the i^{th} cladding mode respectively, α is the attenuation of the cladding mode, θ is the phase difference between the two modes and include a term due to the phase delay introduced by the grating and a term due to the different propagation constants of core mode and cladding modes propagating toward the second grating through the separation length.

The spectral response of a single LPG to SRI changes has been extensively studied [25]. In particular, the effective refractive index of the cladding modes increases as the SRI increases determining a blue shift of the attenuation bands until the SRI reaches the cladding refractive index. At this point there are no longer guided cladding modes and broadband radiation mode coupling occurs. In the case of C-LPGs, the dependence of the cladding modes effective index from the SRI will affect both the position of the envelope of the transmission

#91780 - $15.00 USD Received 15 Jan 2008; revised 13 Mar 2008; accepted 15 Mar 2008; published 18 Jun 2008

spectrum and the position of the interference fringes within the envelope. In fact the change of the cladding modes effective index will change also the phase delay cumulated through the interferometer cavity determining an additional blue shift of the interference fringes [26].

When overlays with higher refractive index compared to the cladding one are deposited along the grating region, refraction-reflection regime at the cladding-overlay interface occurs and the new cladding modes become bounded within the structure comprising the core, the cladding and the overlay. In particular, the overlay deposition leads to a lowering of the cladding mode power bounded within the core and cladding layers, while part of the light power carried by the cladding modes moves toward the HRI overlay determining also the enhancing of the evanescent wave interaction with the surrounding medium and a consequent increased sensitivity of the device to the SRI changes [5]. Moreover the thin HRI overlay itself constitutes a waveguide and allows modes propagation depending on its thickness, refractive index and SRI. In HRI coated LPGs as the SRI increases the lowest order cladding mode is subject to the transition from a cladding mode to an overlay mode with a consequent re-organization of higher order cladding modes. The high sensitivity region of the coated device can be tuned over the desired SRI range by acting on the overlay thickness [6,15].

The numerical analysis of coated UV-LPGs was already reported [5, 27] and has been shown to qualitatively hold in the case of coated TLPGs [15]. The aim of this work is to exploit the enhanced sensitivity of coated LPGs combined with the higher resolution offered by the finer details present in the spectrum of C-LPGs fabricated with the flexible and low cost technique of the arc-discharge.

3. Device fabrication and overlay deposition

The C-TLPGs for our experiments were manufactured from Corning SMF-28 optical fibers, using a computer-assisted precision arc-discharge apparatus. The method is based on periodic melting of the fiber, while a pulling weight stretches it, to determine a periodically tapered fiber. A SEM image of a bare TLPG is reported in Fig. 1 (in the inset) along with the arc-discharge apparatus scheme. The grating period Λ was about 750 μm and was mainly determined by the moving step of the translation stage controlled by a computer, and by some other factors such as arc volume, arc intensity, arc duration time, and pulling weight [14]. After the realization of the first TLPG, whose length was about 2.5 cm, a separation length of about 4 cm was left before the realization of a second grating. On line monitoring of the writing process allows to stop the writing of the second grating once good spectral properties of the C-TLPG are obtained.

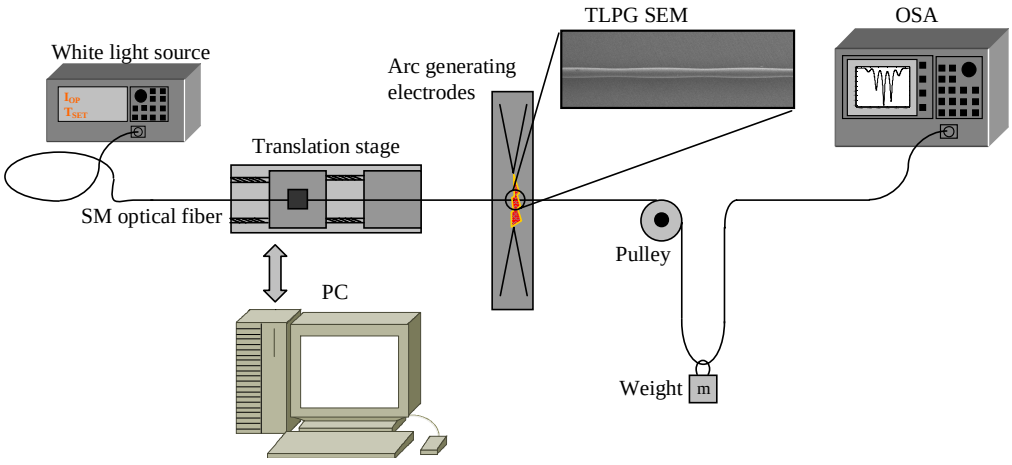

Fig. 1. Computer-assisted arc-discharge apparatus.

#91780 - $15.00 USD Received 15 Jan 2008; revised 13 Mar 2008; accepted 15 Mar 2008; published 18 Jun 2008

The dip-coating technique was used to deposit thin films of sPS (Questra 101 supplied by Dow Chemical Co.), whose refractive index is 1.578 [28], onto the device. This deposition technique consists mainly of immersing the fiber-substrate into a chloroform solution of the polymer and then of withdrawing it with a well controlled speed. The film thickness depends upon many parameters such as the withdrawal speed, the solid content and the viscosity of the liquid. If the withdrawal speed is chosen such that the shear rates keep the system in the Newtonian regime, then the coating thickness depends upon the aforementioned parameters by the Landau-Levich equation [29]. The deposition operations were completely automated by a computerized control system which permitted a constant withdrawal speed of 10 cm/min, thus ensuring the formation of a conformal coating of uniform thickness on the device. A 9% solution by weight of sPS in chloroform was used for the deposition of the overlays onto the C-TLPG. In Fig. 2(a) is reported an optical microscope image (objective magnification 10x) of a coated TLPG. From this image is possible to note the presence of the overlay on the device. In Fig. 2(b) a lower objective magnification (5x) was used to give a better overview of the coated device, in this case the focus is on the surface of the fiber in order to highlight the presence of the overlay, instead the image in Fig. 2(c) is focused on the edges of the TLPG to show that no macroscopic amassment of polymeric material is present in the waist of the tapered region. In order to perform a direct measurement of the overlay thickness by Atomic Force Microscopy (AFM), a sharp blade was used to scratch the overlay. In Fig. 2(d) is reported another optical image (objective magnification 10x) of the scratched overlay. Also from this last image there is no evidence of overlay thickness disuniformity.

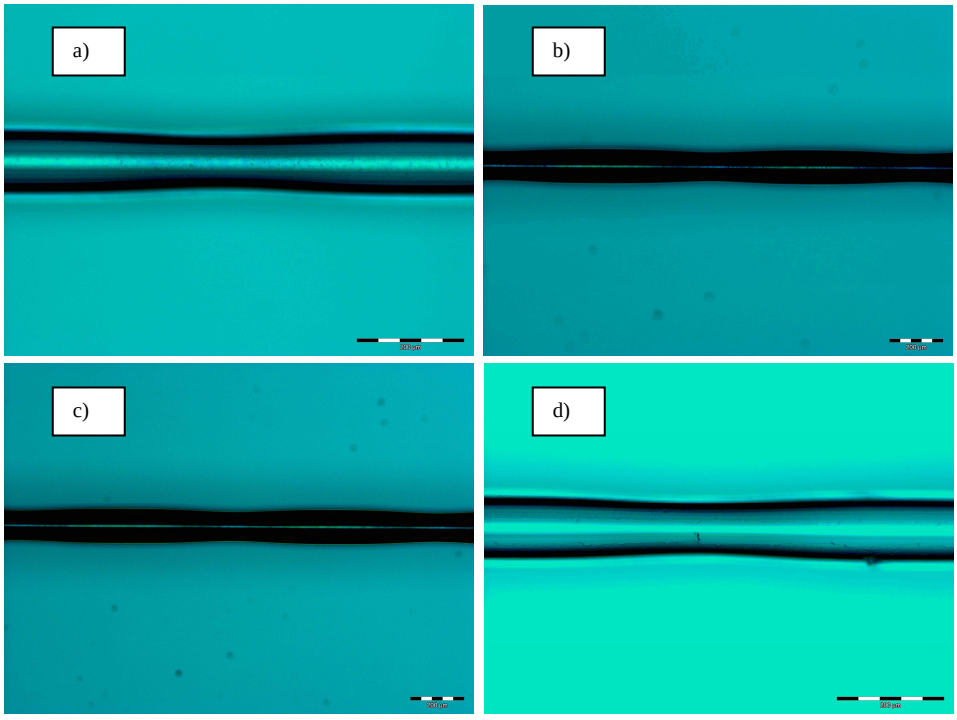

Fig. 2. (a) Coated TLPG (10x objective magnification);(b) overview of the coated TLPG (5x objective magnification, focus on the surface); (c) overview of the coated TLPG (5x objective magnification, focus on the edges); (d) scratched overlay for following AFM measurements (10x objective magnification).

Finally AFM characterization of the scratched overlay was performed and the results are shown in Fig. 3 with a 12x12 μm^2 topography image, the straight line and the markers are related to the cross section of the topography which is shown in Fig. 4. It is worth to note that

#91780 - $15.00 USD Received 15 Jan 2008; revised 13 Mar 2008; accepted 15 Mar 2008; published 18 Jun 2008

the curvature of the fiber in this last image is exaggerated due to the different scales of the axis. For this reason a good measure of the overlay thickness is just the difference of the ordinates of the two markers, which is in this case about 320 nm. The overshoot of the profile next to the trench wall is always present when removing material and should not be taken into account for the measurement of the overlay thickness. Different measurements of the overlay thickness in different regions of the coated device permitted to conclude that the overlay thickness was 315 nm +/-10 nm.

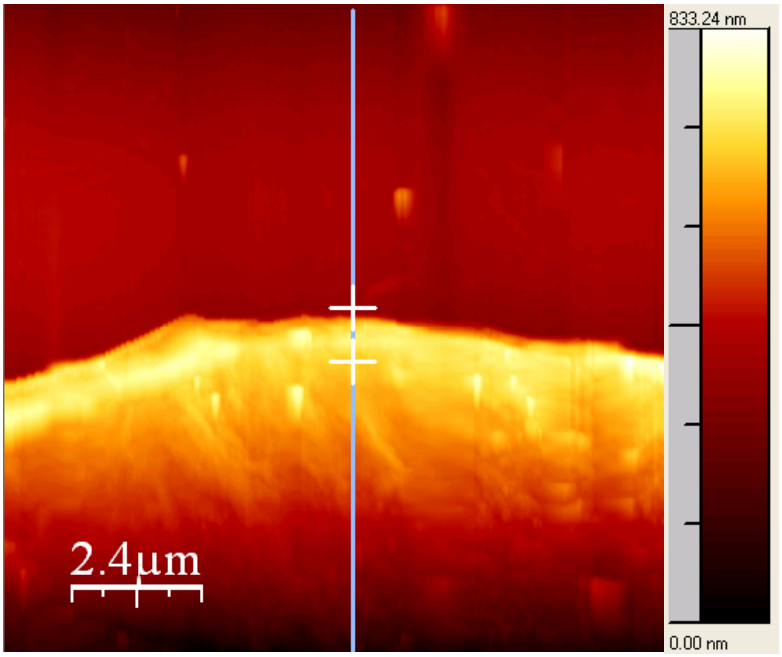

Fig. 3. AFM topography image (12x12 µm^2) of the scratched overlay onto the TLPG. Line and markers are referred to the cross section reported in Fig. 4.

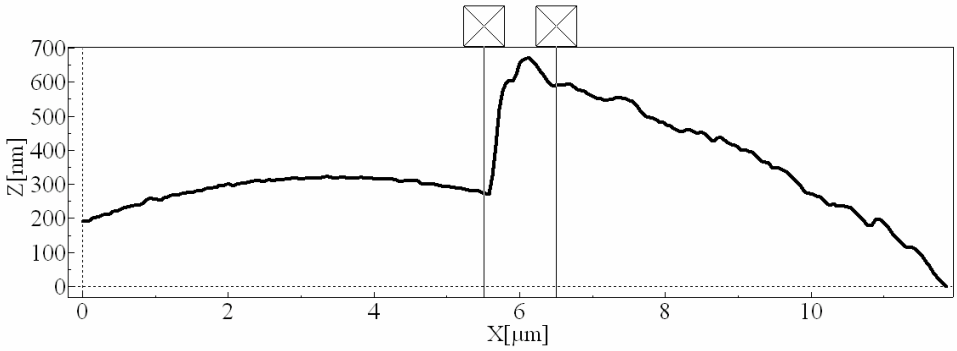

Fig. 4. Cross section of the measured topography. Overlay thickness is measured to be about 320 nm in this case.

Three different configurations in terms of coated/not coated areas of the C-TLPG were studied: 1) all coated device, both gratings and separation length; 2) coated separation length and bare gratings; 3) coated gratings and bare separation length. They are summarized in Fig. 5. In particular the last two configurations were realized by coating separately the different components and then splicing them to obtain the compound structure.

#91780 - $15.00 USD Received 15 Jan 2008; revised 13 Mar 2008; accepted 15 Mar 2008; published 18 Jun 2008

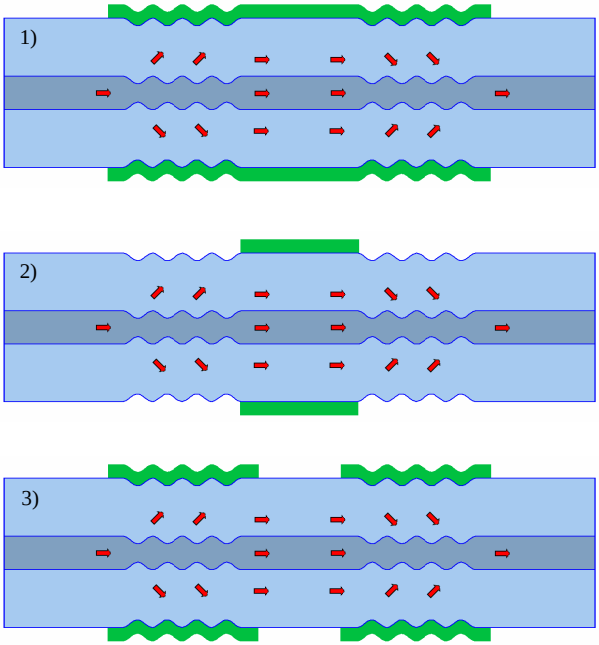

Fig. 5. Summary of the three configurations studied in this work (not to scale): 1) all coated device; 2) coated separation length and bare gratings; 3) coated gratings and bare separation length.

4. Experimental results

The investigation of the thin film coated C-TLPG under test consisted of recording its transmission spectra for different SRI values in each of the aforementioned configurations starting from the bare device. The optoelectronic set-up used for SRI characterization comprises a white light source of 400-1800 nm wavelength range and an optical spectrum analyzer. The analysis was focused on the spectral range 1450 – 1700 nm. The SRI was changed by using aqueous glycerol solutions whose refractive indices were measured by an Abbe refractometer at 589 nm.

The measurements were performed at room temperature with an air conditioning system as the only mean to keep the temperature as constant as possible. Each experiment lasted less than 2 hours so that a couple of °C of variation in the temperature can not be excluded. Therefore a temperature-induced error in the wavelength shifts reported in this work has to be presumed. However this work was not intended to be an accurate measurement of the SRIs, but instead to suggest a way to improve the performance of cascaded LPGs when used as refractometer or as chemical sensor. When an accurate measurement has to be performed it is necessary to use an accurate control of the temperature or suitable compensation methods.

The temperature cross-sensitivity will be discussed in a next subsection, but we can anticipate that temperature fluctuations affecting measurements considered here are not able to modify the trend of the SRI sensitivity characteristic of the coated C-TLPG.

4.1 Bare C-TLPG

The SRI characterization carried out for the bare C-TLPG is presented in Fig. 6. The spectra present three main attenuation bands due to coupling of the fundamental core mode (LP_{01}) with low order cladding modes ($LP_{0i,}$ i=2-4) performed by the first grating. Those attenuation bands are the envelope of interference fringes due to re-coupling of cladding light into the core, determined by the second grating, and to the consequent interference with the core light.

#91780 - $15.00 USD Received 15 Jan 2008; revised 13 Mar 2008; accepted 15 Mar 2008; published 18 Jun 2008

It is observable in Fig. 6(a) that as the SRI value increases, both the envelopes and each interference fringe within them experience a small blue shift with a slight reduction of the fringe visibility.

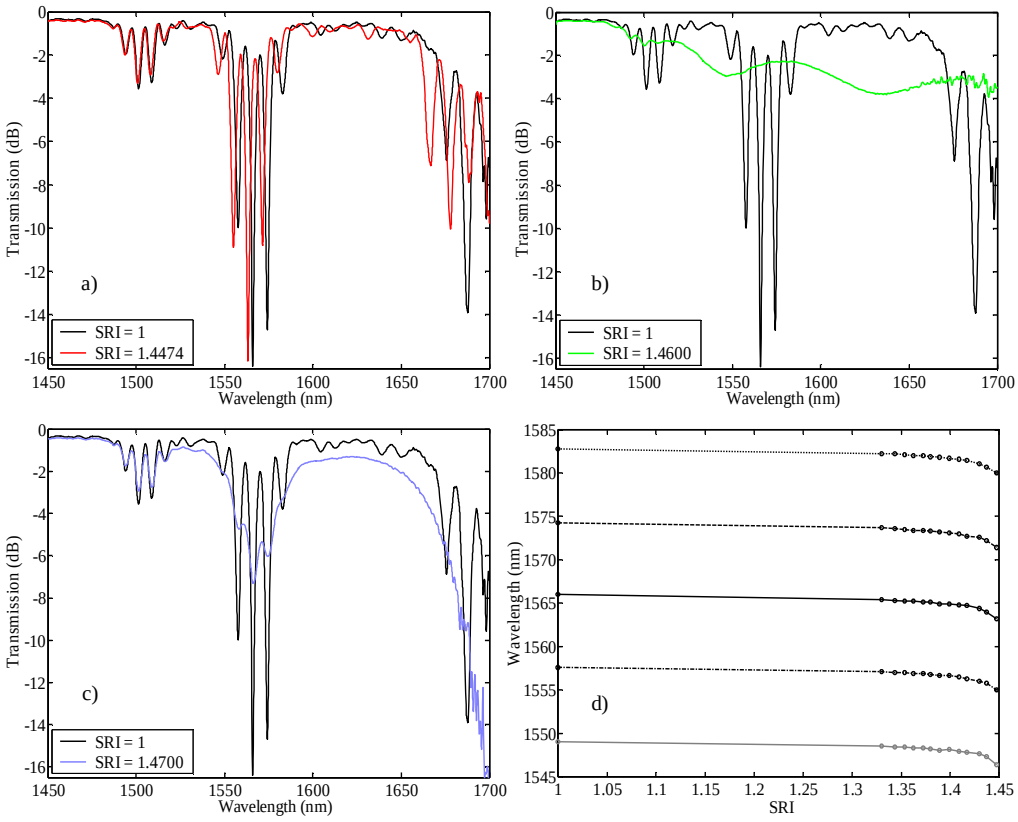

Fig. 6. Spectral characterization to SRI changes of the bare C-TLPG under test: (a) guided cladding modes; (b) broadband radiation modes; (c) leaky modes; (d) wavelength shift of the interference fringes related to cladding mode LP_{03}.

The fringes shift is consistent with Eq. (1) , since the higher the SRI the higher the effective refractive index of the i^{th} cladding mode, and with Eq. (2), since the increasing of the cladding modes effective index determines a reduction of the optical path difference thus ensuring the same phase difference θ, and hence intensity, for shorter wavelengths (fringes phase shift). As the SRI value approaches the cladding refractive index (Fig. 6(b)), the optical fiber is not able to guide anymore discrete cladding modes and broadband radiation mode coupling occurs. In this case the transmission spectrum is given by the sum of the broadband losses generated separately by the two gratings. In fact for SRI=1.4600 no interference fringes are visible at all and broad attenuation bands are significantly blue shifted. The transmission spectrum of the device for SRI=1 as been kept in all the plots as a reference. For higher SRIs (Fig. 6(c)) the presence of leaky modes determines the attenuation bands and interference fringes reappearance at higher wavelengths with increasing visibility but with almost no sensitivity in terms of wavelength shift to SRI changes. In Fig. 6(d) is reported the wavelength shift experienced by the interference fringes minima present in the attenuation band related to the cladding mode LP_{03} when the SRI changes. It is worth noting that this wavelength shift is the sum of two contributions: 1) the shift of the attenuation band envelope attributable to the behavior of the gratings considered as isolated elements; 2) the fringes phase shift due to the change of the cladding modes optical path in the sepataration length.

#91780 - $15.00 USD Received 15 Jan 2008; revised 13 Mar 2008; accepted 15 Mar 2008; published 18 Jun 2008

4.2 All coated C-TLPG

The spectral behaviour of the C-TLPG under test coated with a polymeric overlay deposited on both gratings and on the separation length between them was investigated. As already mentioned, the overlay was obtained from a 9% solution of sPS in chloroform, and the overlay thickness was evaluated to be approximately 315 nm. When an HRI overlay is deposited onto the grating the effective refractive index of the cladding modes is increased, as a consequence both the attenuation bands and interference fringes experience a blue shift. This is clearly observed in Fig. 7. where the attention has been focused on the LP_{03} interference fringes in the spectral range 1530-1600 nm.

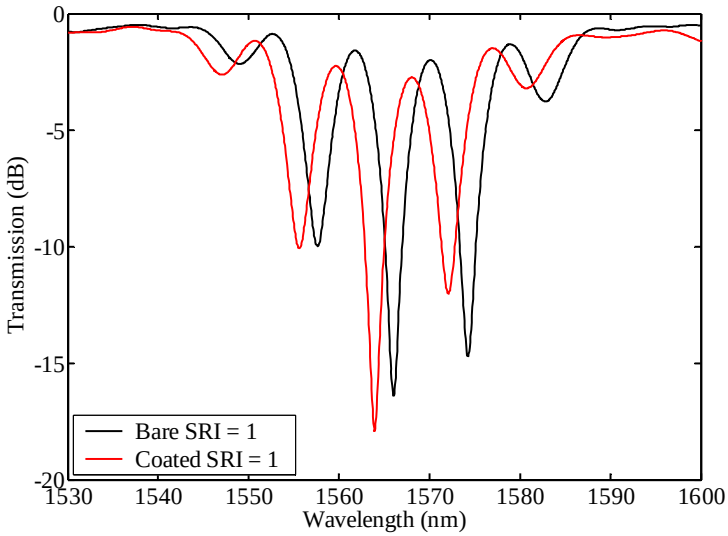

Fig. 7. Shift of the interference fringes related to the cladding mode LP_{03} caused by the deposition of an sPS overlay of about 315 nm.

The SRI characterization is shown in Fig. 8. There it is observable that the attenuation bands as well as the interference fringes shift to shorter wavelengths as the SRI increases with increased sensitivity ($\partial\lambda/\partial SRI$) compared to the bare device (Fig. 8(a)). However the fringes visibility decrease faster with respect to the SRI and goes to zero for n= 1.3624 (Fig. 8(b)). For higher SRIs the modal transition of the lowest order cladding mode into an overlay mode takes place along with the consequent modal re-organization. The attenuation bands shift to recover the position of the next lower attenuation band without interference fringes which start to reappear with increasing visibility at the end of the modal re-organization (Fig. 8(c)).
Differently from the case of the bare device, the HRI overlay prevents the matching of the cladding refractive index with the SRI thus "shielding" the cladding modes against the radiation mode coupling and extending the measurable wavelength shift of the attenuation bands to SRIs higher than the cladding one. The fringes visibility reduction is due to an increased attenuation of the cladding modes during the modal re-organization. In fact it was shown by del Villar et al. [10] that when there is the maximum cladding mode power content in the overlay there is also a maximum of the imaginary part of the cladding modes propagation constants. This explanation was invoked to justify the attenuation band vanishing in coated LPGs with overlays deposited by ESA technique. Although the dip-coating technique permits to deposit low loss overlays, as clearly understandable by the fact that the attenuation bands remain visible during the modal re-organization, nonetheless some amount of loss is present also in this case as suggested by the notable reduction of the attenuation bands depth during the modal re-organization.

#91780 - $15.00 USD Received 15 Jan 2008; revised 13 Mar 2008; accepted 15 Mar 2008; published 18 Jun 2008

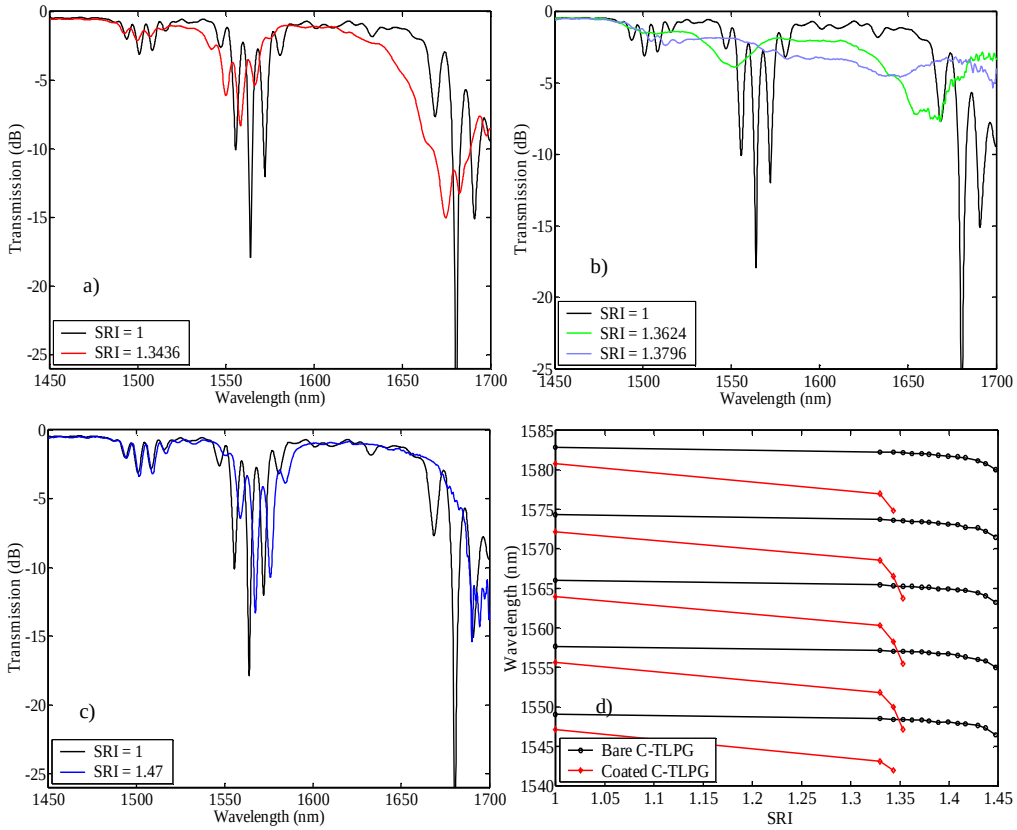

Fig. 8. Spectral characterization of the all coated C-TLPGs in different points of the SRI induced modal transition: (a) beginning; (b) half-way; (c) toward completion; (d) comparison of the LP_{03} interference fringes minima wavelength shift in the bare and all coated C-TLPGs.

In Fig. 8(d) is reported a comparison between the wavelength shift of the interference fringes minima related to the cladding mode LP_{03} of the bare device and that shift in the coated device. That plot shows an increased sensitivity of the coated device which could be exploitable for a sensor until the interference fringes disappear. Moreover, the high sensitivity region of the device can be tuned in the desired SRI range by changing the overlay thickness as already shown for single TLPGs in [15]. In particular, there it was reported that the deposition of an overlay from a 9% solution by weight of sPS tunes the peak of the TLPG sensitivity characteristic around a SRI=1.363. Here also the highest sensitivities are achieved around the same SRI, thus confirming the high reproducibility of the overlay thicknesses deposited with well controlled parameters of the dip-coating process. Finally, it is easily arguable, again from a comparison with the data reported in [15], that increasing the overlay thickness by means of a deposition from higher concentration solutions it is possibile to increase the sensitivity of the bare device in SRI ranges where it is usually very poor (e.g. SRI=1) but which are interesting for sensing applications (chemical sensing in gaseous environment). In order to clarify where, along the device, the presence of the coating is most critical for the emergence of the drawback of the fringes visibility reduction and to extend the SRI range over which the fringes remain visible, other configurations were studied.

4.3 Coated separation length, bare TLPGs

The SRI characterization was repeated for the C-TLPG under test after having accurately removed the previously deposited overlay in boiling chloroform and having deposited a new overlay just on the separation length between the two gratings. The same deposition

#91780 - $15.00 USD Received 15 Jan 2008; revised 13 Mar 2008; accepted 15 Mar 2008; published 18 Jun 2008

parameters were used. In this case the attenuation bands position has the same dependence on the SRI changes as in the case of the bare device. Therefore, a reduced overall sensitivity to SRI changes is expected compared to the previous case since for the cladding modes in the bare gratings there is no modal transition. Instead the propagation constants of the cladding modes in the separation length are increased along with their sensitivity to the SRI changes and the mechanism of the modal transition is allowed in this length. In fact a greater sensitivity in terms of interference fringes phase shift to SRI changes is found with regard to the bare C-TLPG. From Fig. 9(a) it is possible to retrieve that for a SRI=1.3436 the inteference fringes minima are already at shorter wavelengths than those at which they are for a SRI= 1.4474 in the bare C-TLPG (Fig. 6(a)). For higher SRIs the fringes visibility was dramatically reduced to zero with a similar behavior to the previous case (Fig. 9(b)). However this phenomenon suggested that the presence of the overlay on the separation length is the main responsible for the reduction of the fringe visibility in the SRI range in which the modal transition takes place. It is important to stress that the modal transition here is possible exclusively in the coated separation length, this obviously leads to a higher SRI sensitivity in terms of interference fringes shift strongly related to the delay segment between the bare gratings. However, the device demonstrates a reduced SRI sensitivity compared with the previous case due to the limited wavelength shift of the attenuation bands of the bare gratings. It is worth to note that for even higher SRIs, i.e. at the end of the modal transition, the interference fringes appear again (Fig. 9(c)).

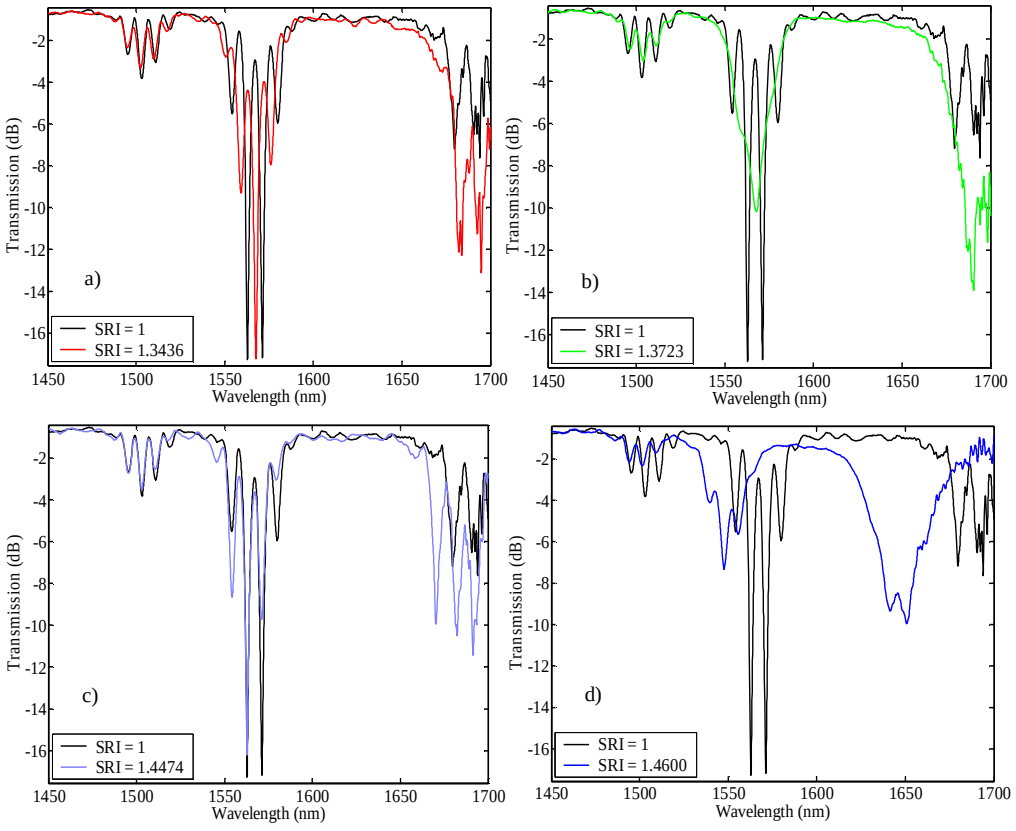

Fig. 9. Spectral characterization of the C-TLPGs with coated separation length and bare gratings in different points of the SRI induced modal transition in the separation length itself: (a) beginning; (b) half-way; (c) toward completion; (d) broadband radiation modes coupling by the bare gratings.

#91780 - $15.00 USD Received 15 Jan 2008; revised 13 Mar 2008; accepted 15 Mar 2008; published 18 Jun 2008

Moreover for SRI=1.4600 (Fig. 9(d)) the attenuation bands are positioned at the same wavelengths as in the corresponding SRI case for the bare device (Fig. 6(b)), but here interference fringes are slightly visible. This happens because the HRI overlay prevent the radiation mode coupling for this SRI in the separation length. In this way the cladding modes power is not totally dissipated and they can arrive on the second grating to interfere with core mode. Also, the coupling efficiency is greater than the bare case as witnessed by the deeper attenuation bands.

Although this case is not very attractive for sensing applications it has served to recognize that the presence of the coating along the separation length is critical to the interference fringes visibility during the modal transition. The next step to confirm this inference was to investigate the device with coated gratings and bare separation length. This configuration, infact, should provide the best performances of the final device since the coated gratings would ensure high SRI sensitivity due to the modal transition mechanism. In addition, the bare separation length should enhance the fringe visibility leading to extended SRI range.

4.4 Coated TLPGs, bare separation length

This case is referred to scheme reported in Fig. 5(3). Once again the overlay was accurately removed from the C-TLPG after the previous characterization and a new overlay was deposited on the two gratings leaving the separation length uncoated. Then, the SRI characterization was performed and reported in Fig. 10.

In this case the attenuation bands shift toward shorter wavelengths for an increasing SRI as expected for a coated LPG. The interference fringes also experience a blue phase shift (within the attenuation band) but, reasonably, with a reduced sensitivity compared to the cases in which the separation length is coated. Moreover the interference fringes are maintained with a good visibility over a wider range of SRIs. This can be clearly appreciated by noting that in Fig. 10.b) the attenuation band related to the cladding mode LP_{04} is in the middle way between its initial position and that of the next lower attenuation band and it still has high fringes visibility. Unfortunately a comparison of the LP_{04} behaviour in all the cases is not possible because in the previous cases this band is placed at higher wavelengths where the high noise level of the light source does not allow a good retrieving of its spectral characteristics. For higher SRIs (Fig. 10(c)) the modal re-organization goes towards its completion. In Fig. 10(d) is reported a comparison of the interference fringes wavelength shift related to cladding mode LP_{03} between the cases of the all coated device and the coated gratings with bare separation length. For this comparison the cladding mode LP_{03} has been followed during all the transition to the position of the LP_{02}.

As already mentioned the interference fringe visibility decreases slower with the SRI in the case treated here, and in fact this permits to have more points in the relative graph in Fig. 7(d). The behavior of the visibility is more clear in Fig. 10(e), where it is calculated as $V = (T_{\min}^{upp} - T_{\min}^{low})/(T_{\min}^{upp} + T_{\min}^{low})$, with $T_{\min}^{upp}$ and $T_{\min}^{low}$ minimum of the upper and lower envelope of the transmittivity respectively. There are again compared the all coated device and the coated gratings with bare separation length cases. The latter starts with a lower visibility, but maintain an higher visibility over a wider range of SRIs. In the middle of the modal re-organization the visibility is not completely zero but is not defined because the spectrum has not a clear shape. At the end of the modal re-organization, this last configuration has lower visibility than the all coated C-TLPG. This is most likely due to the fact that the cladding modes in the bare separation length have a bigger extension in the surrounding medium and hence they arrive at the second grating with less power than in the other case.

This configuration showed the best results in terms of fringes visibility endurance and hence of exploitable sensitivity enhancement. Moreover the sensitivity enhancement is mainly due to the mechanism of the modal transition before to the presence of the interferometer cavity.

#91780 - $15.00 USD Received 15 Jan 2008; revised 13 Mar 2008; accepted 15 Mar 2008; published 18 Jun 2008

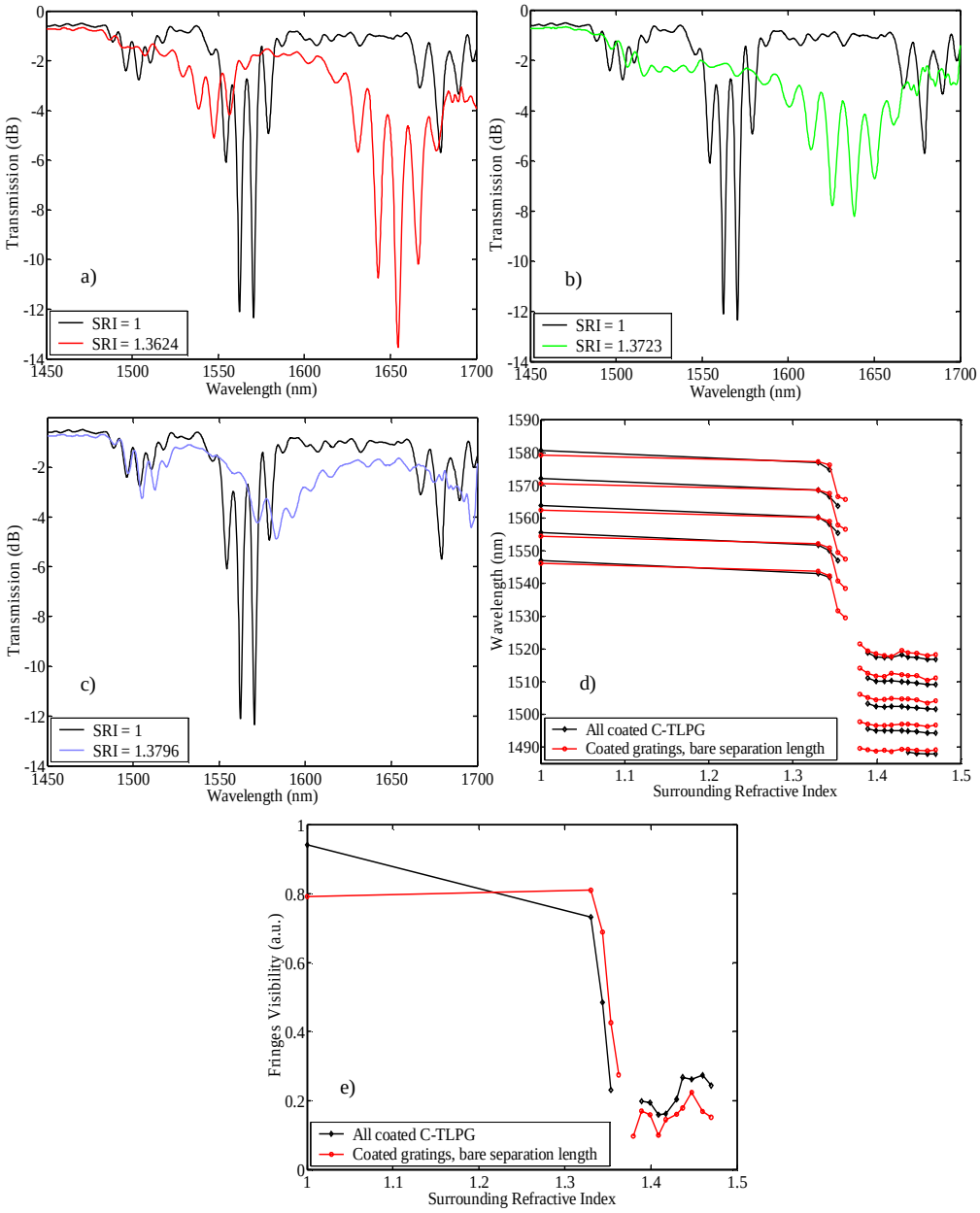

Fig. 10. Spectral characterization of the C-TLPGs with coated gratings and bare separation length in different points of the SRI induced modal transition in the gratings themself: (a) beginning; (b) half-way; (c) toward completion; (d) comparison of the LP_{03} interference fringes minima wavelength shift in the all coated C-TLPGs and in the device with coated gratings and bare separation length; (e) comparison of the fringes visibility in the same cases as in (d).

4.5 Comments on the temperature sensitivity of the presented results

The temperature sensitivity of a bare LPG is function of the thermo-optic coefficient difference of the core and cladding materials, of the coupled cladding mode and of the wavelength at which the specific mode is fed by the core power, or in other words of the

#91780 - $15.00 USD Received 15 Jan 2008; revised 13 Mar 2008; accepted 15 Mar 2008; published 18 Jun 2008

grating period [30]. The phenomenon is even more complex when the LPG is coated by a thin overlay and the surrounding medium in not air. For these reasons a detailed analysis of the temperature sensitivity of the proposed device is complex and is behind the scope of this work. However rough estimations of the temperature sensitivity can still be given. For low order cladding modes of a LPG written in SMF-28 fibers, with air as surrounding medium, temperature sensitivities ranging from 0.05 to 0.1 nm/°C have been reported in literature [31]. When a bare LPG is used as refractometer, the non-linear behaviour of its sensitivity to SRI changes and the thermo-optic coefficient of the surrounding medium should be considered. In fact for low SRIs the intrinsic temperature sensitivity of the bare LPG is prevailing, whilst for SRIs reaching the refractive index of the cladding material the temperature-induced refractive index change of the surrounding medium becomes more important [32].

A SRI of about 1.46 can be obtained with a water/glycerine mixture in a weight percentage of about 10/90 %. The SRI sensitivity around this index for the LP_{03} of a bare TLPG is between 500 and 1000 nm/refractive index unit (RIU) [15]. Assuming a thermo-optic coefficient of $2.2*10^{-4}$ for the glycerine and $1*10^{-4}$ for the water [33], a thermo-optic coefficient of the surrounding medium of about $2*10^{-4}$ is obtained. This means a temperature sensitivity of 0.1-0.2 nm/°C plus the intrinsic grating temperature sensitivity.

For a coated LPG the sensitivity characteristic to SRI changes is modified with respect to a bare LPG, having a resonant shape with the maximum in correspondence of the refractive index for which there is the transition of lowest order cladding mode and the consequent cladding mode re-organization [6]. Also the sensitivity to the refractive index changes of the overlay has the same resonant shape as function of the SRI [8]. In this case also the thermo-optic coefficient of the coating material should be considered and for the sPS it can be assumed to be $4*10^{*-4}$ [28]. The maximum sensitivity to the overlay refractive index changes for the LP_{03} can be estimated to be about 4500 nm/RIU (in the case treated in this work with an overlay thickness of about 315 nm, at an SRI≈1.36 and at $\lambda \approx 1550$ nm) while the maximum sensitivity to SRI changes is about 3 times smaller. These high sensitivities are due to the high content of the field in the overlay and in the surrounding medium during the modal re-organization, and the difference between the two sensitivities is because the field confinement factor is much higher for the overlay compared to the surrounding medium.

In this situation a temperature sensitivity, due to the temperature-induced overlay index change, of about 1.8 nm/°C can be calculated. A SRI of about 1.36 can be obtained with a water/glycerine mixture in a weight percentage of about 80/20 % so that a thermo-optic coefficient of about $1.2*10^{-4}$ can be assumed for the surrounding medium. This means that the total temperature sensitivity in the middle of the transition region can be as high as 2 nm/°C. However it is worth to note that a material for chemical sensing applications such as the sPS can undergo an index change of the order of 10^{-2} in response to the presence of few ppm of analyte in the surrounding medium [8,28]. In this case the temperature-induced error in the measurement of the wavelength shift would be of about 1%/°C.

Considering cascaded LPGs also the optical delay line plays a role in the temperature sensitivity. However we consider just the third case (coated LPGs and bare separation length) being the most effective for sensing purposes. In this case the temperature sensitivity plus due to the bare interferometer cavity is two orders of magnitude less than that of the coated LPG [34] , so that the major role is just played by the latter.

5. Conclusions

In this work HRI coated C-TLPGs have been investigated in order to obtain devices with increased SRI sensitivity and higher resolution through the presence of finer scale features in the transmission spectrum. The most trivial configuration, all coated device, while increasing the SRI sensitivity of the bare device has shown to be affected by a fast disappearing of the interference fringes. Different configurations, in terms of coated/not coated areas, were investigated to the aim of rejecting this drawback. The presence of the coating on the separation length has been recognized as the principal reason for the cladding modes attenuation during the cladding modes re-organization and consequently of the fringe

#91780 - $15.00 USD Received 15 Jan 2008; revised 13 Mar 2008; accepted 15 Mar 2008; published 18 Jun 2008

visibility annulment The best results in terms of increased sensitivity and extended SRI working range were obtained when the gratings were coated while the separation length was bare. However, also in this case it was not possible to completely maintain the fringe visibility during the modal re-organization, but this time the fringe visibility resulted to be not defined due to a not clear shape of the spectrum. This is most likely due to a non-synchronized movement of the attenuation bands of the two gratings with the SRI. In fact the two gratings of the C-TLPG while being very similar are not equal and also the coating thickness can change few nanometers from one grating to another further enhancing the differences in the middle of the modal re-organization. From this work some considerations on future developments can be derived. The adoption of a reflection mode cascaded configuration, also named Michelson configuration, can solve the problem of the differences between the two gratings giving at the same time a compact probe. Further improvements of the device could be achieved through a careful design of the separation length and of the power transfer to a specific cladding mode that one wish to interrogate.

Acknowledgments

Canadian authors gratefully acknowledge Canada's NSERC and CFI for financial support. The C-TLPGs were fabricated by Mr. P. Mikulic at the Centre de recherche en photonique, UQO.

#91780 - $15.00 USD Received 15 Jan 2008; revised 13 Mar 2008; accepted 15 Mar 2008; published 18 Jun 2008